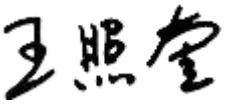
创新创业学分认定诚信声明

本人郑重声明：所提交的用以申请创新创业学分认定的内容(包括但不限于学科竞赛获奖、学术论文、科研项目成果、专利创造成果、文学艺术类成果以及创业实践类成果等)均为本人在校期间原创取得，不存在任何侵权、造假等违规行为。

本人完全意识到本声明的法律后果由本人承担。本人所提交的内容如涉嫌违规违法，本人愿意承担相应后果。

申请人签名：

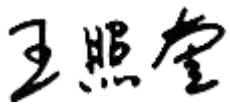
指导（证明）老师签名：

2025年6月3日

推荐信

学生王少奇在课题组内积极学习，认真实验，最终提炼出使用芬那露对蓝色准二维钙钛矿薄膜进行优化。在同门的帮助下完成所有实验，并将相关论文发表在期刊 *Chemical Engineering Journal*。论文数据真实可靠，课题明了有创新。

推荐人：王照奎 教授



2025 年 6 月 6 日

推荐信

针对目前蓝色 PeLEDs 的寿命和稳定性问题，学生王少奇利用添加剂芬那露的 C=O 和 S=O 钝化不饱和 Pb^{2+}，抑制薄膜分解；并通过控制钙钛矿晶体的结晶动力学改善薄膜形貌。最终实现器件寿命和稳定性的双提高。最终发表在期刊 *Chemical Engineering Journal*。有资格申请创新创业学分认定。

推荐人：王雪东 教授

王雪东

2025 年 6 月 6 日

检 索 报 告

苏州大学图书馆　　报告编号：**2025suda0644**

受苏州大学纳米科学技术学院王少奇委托，检索其提交的论文在SCI-EXPANDED数据库收录情况。

检索情况及其结果：

检索类别：SCI-E 收录

检索方式：机检

检索范围：国外

检索工具：SCI-EXPANDED

检索时限：2025年

检索人：张禾

检索结果：

1. 苏州大学王少奇提交的文章在2025年间有 1 篇论文被 SCI-EXPANDED 收录，收录详情见附件。

苏州大学科技查新工作站

2025年6月4日

附件一：收录文献

#	收录文献	数据库
1	标题: **Dual Channel passivation enhancing stable perovskite Light-Emitting diodes** 作者: **Wang, SQ (Wang, Shao-Qi)**; Yang, W (Yang, Wei); Xia, Y (Xia, Yu); Wang, B (Wang, Bin); Li, N (Li, Nan); Huang, L (Huang, Lei); Chen, X (Chen, Xin); Li, YH (Li, Yu-Han); Chen, J (Chen, Jing); Chen, CH (Chen, Chun-Hao); Wang, ZK (Wang, Zhao-Kui) 地址: [Wang, Shao-Qi; Yang, Wei; Xia, Yu; Wang, Bin; Li, Nan; Huang, Lei; Chen, Xin; Li, Yu-Han; Chen, Jing; Chen, Chun-Hao; Wang, Zhao-Kui] Soochow Univ, Inst Funct Nano & Soft Mat FUNSOM, Jiangsu Key Lab Adv Negat Carbon Technol, Suzhou 215123, Jiangsu, Peoples R China. 通讯作者: Wang, ZK 来源出版物: *CHEMICAL ENGINEERING JOURNAL* 卷: 505 文献号: 159796 提前访问日期: JAN 2025 出版年: 2025 出版时间: FEB 1 入藏号: WOS:001408345800001 出版物类型: J 文献类型: Article	SCI-EXPANDED

End

Chemical Engineering Journal 505 (2025) 159796

Contents lists available at ScienceDirect

Chemical Engineering Journal

journal homepage: www.elsevier.com/locate/cej

Dual Channel passivation enhancing stable perovskite Light-Emitting diodes

Shao-Qi Wang, Wei Yang, Yu Xia, Bin Wang, Nan Li, Lei Huang, Xin Chen, Yu-Han Li, Jing Chen, Chun-Hao Chen, Zhao-Kui Wang *

Institute of Functional Nano & Soft Materials (FUNSOM), Jiangsu Key Laboratory of Advanced Negative Carbon Technologies, Soochow University, Suzhou, Jiangsu 215123, China

ARTICLE INFO

Keywords:
Perovskite LEDs
Passivation
Stability

ABSTRACT

Perovskite light-emitting diodes (PeLEDs) still faces the challenges such as poor film morphology and inefficient energy transfer from the small-n phase to the large-n phase leading to rapid efficiency degradation and instability in high temperature. To address these issues, herein, chlormezanone was employed to modify the perovskite film. Combined beneficial points were obtained including improved film morphology, reduced luminescence quenching, enhanced phase distribution and energy transfer by suppressing small-n phases, and defect mitigation at grain boundaries/interfaces via passivation groups (C = O, S = O). Consequently, the fabricated sky-blue PeLEDs delivered an external quantum efficiency of 10.14 % and an operating lifetime (T_{50}) of 23.1 min, which was twice as long as the control device. This developed strategy significantly enhanced the stability while maintain excellent efficiency, providing a solid foundation for future investigation.

1. Introduction

Metal halide perovskite materials have demonstrated significant potential in the realms of display and lighting, owing to their exceptional photoelectric properties, rendering them as highly promising materials for next-generation luminescence [1–5]. In recent years, the external quantum efficiency (EQE) of perovskite light-emitting diodes (PeLEDs) has surpassed 20 % for red and blue emissions and exceeded 30 % for green emissions, marking substantial progress comparable to OLEDs [6–8]. However, blue-emitting PeLEDs face challenges such as rapid efficiency degradation, unstable luminous color, and short lifetimes [9–11]. Despite achieving efficiency levels on par with other color emissions, attaining high stability and prolonged lifetime for blue light remains challenge due to the elevated defect density at perovskite grain boundaries and surfaces, leading to pronounced non-radiative recombination. These issues have influenced the application and progress of perovskite lighting and display technology [12–16].

Additives are the most common method for passivating perovskite defects [5,17–19]. Lewis base molecules, incorporating certain functional groups, have been reported to saturate halide vacancies within perovskite membranes by sharing lone-pair electrons with the vacant orbitals of lead ions, effectively mitigating defects on perovskite surfaces and grain boundaries [10,19–24]. In 2021, Li *et al.* studied adding TMOS to perovskite solution. Methoxylation of TMOS passivated under − coordinated Pb^{2+} ions, reducing non − radiative recombination and enhancing the PCE of perovskite solar cells by nearly 3 % [24]. Similarly, in 2023, Sun *et al.* employed formamidine sulfinic acid to optimize green PeLEDs. Leveraging the sulfur-oxygen double bond, carbon–nitrogen double bond, and amino group of the organic molecule, they achieved significant improvements in device efficiency [25]. In 2023, Yu *et al.* elucidated the passivation mechanism of diphenylphosphine oxide (DPPA) molecules on perovskite surfaces. Using this molecule, they extended device lifetime by 32 % [26].

In this study, we conducted a comprehensive investigation into the impact of the organic additive chlormezanone on modifying quasi-2D perovskite films. Through the modification of the perovskite emissive layer (EML) with multifunctional group additives, we effectively enhanced the film morphology, resulting in the preparation of a more uniform and dense film that mitigates the detrimental effects of leakage current on device performance. Furthermore, this approach proved effective in suppressing the formation of small-n phases and facilitating efficient energy transfer from small-n phases to large-n phases, thereby playing a pivotal role in achieving high-performance PeLEDs. Importantly, this method demonstrated the capability to significantly reduce

* Corresponding author.
E-mail address: zkwang@suda.edu.cn (Z.-K. Wang).

https://doi.org/10.1016/j.cej.2025.159796
Received 6 December 2024; Received in revised form 16 January 2025; Accepted 20 January 2025
Available online 22 January 2025
1385-8947/© 2025 Published by Elsevier B.V.

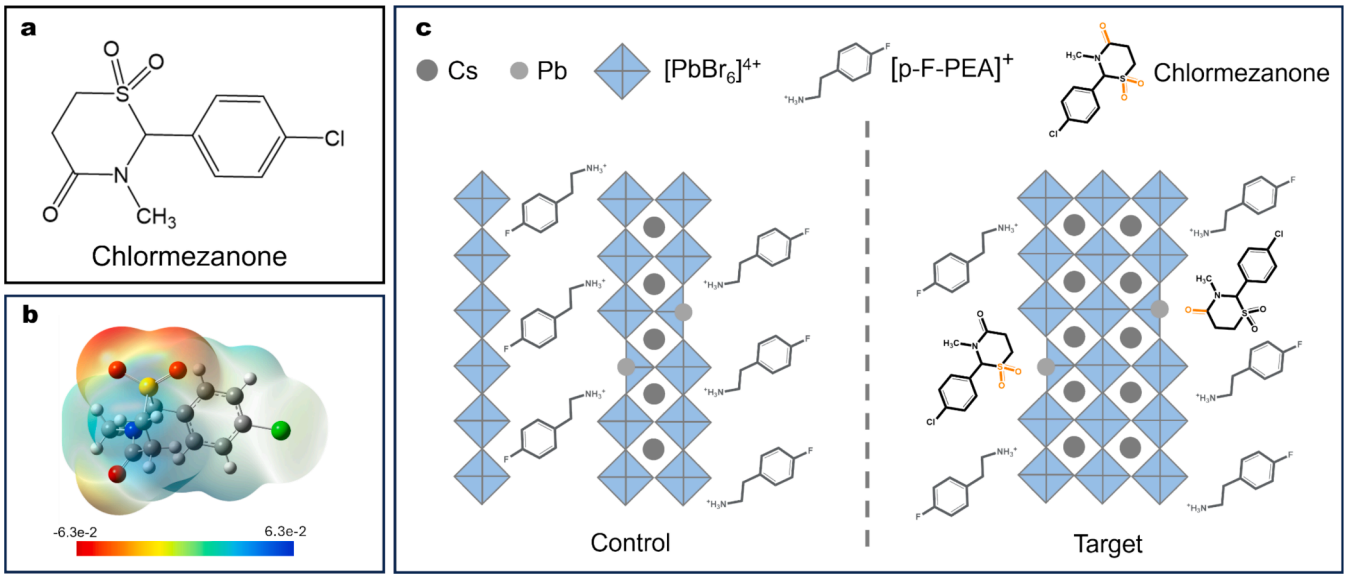


Fig. 1. (a) The molecular formula of chlormezanone. (b) Electrostatic potential (ESP) distribution of the chlormezanone molecule. (c) Schematic diagram of regulatory phase distribution and crystal crystallization.

the density of trap states and inhabit the decomposition of the film, especially at high temperatures. As a result, we successfully extended the lifetime of the PeLED emitting at 486 nm to 23.1 min, doubling the time compared to the control device. Remarkably, even under these the performance, the prepared device maintained an external quantum efficiency of 10.14 %. This method enhanced the electroluminescence and photoluminescence performance of the film and provided a solid foundation for further research on sky-blue PeLEDs to achieve a better performance.

2. Materials and methods

2.1. Materials

Cesium bromide (CsBr, 99.0 %), lead bromide ($PbBr_2$, 99.0 %), lead chloride ($PbCl_2$, 99.0 %), dimethyl sulfoxide (DMSO), chlorobenzene (CB), and formamidine bromide (FABr, 99.0 %) were obtained from Sigma-Aldrich. From Xi'an Polymer light technology Corp, 4-Fluorophenylethylammonium bromide (p-F-PEABr, 99.5 %), TPBi (99.9 %), and Liq were purchased. Acros supplied poly (9-vinylcarbazole) (PVK) and chlormezanone (99.0 %). Without further purification, all the materials were used directly as received

2.2. Fabrication of perovskite film

The precursor solutions were obtained by dissolving CsBr (0.12 M), $PbBr_2$ (0.06 M), and $PbCl_2$ (0.06 M) in DMSO. Additionally, p-F-PEABr (0.03 M), LiBr (0.014 M), and FABr (0.01 M) were incorporated into the precursor solutions as additives. The difference between the target and the control was determined by the presence or absence of chlormezanone (0.01 M, which is depended by the Fig. S1). Before use, the precursor solutions were stirred in a nitrogen-filled glove box at room temperature for 30 min until fully dissolved. The perovskite films were then formed by spin-coating the precursor solutions onto PVK-coated ITO substrates at 4000 rpm for 140 s. After spin-coating, the perovskite films in their wet states were annealed at 65 °C for 5 min or another designated time

2.3. Devices fabrication

PeLEDs were fabricated with a structure consisting of ITO/PVK/perovskite/TPBi/Liq/Al. Initially, ITO-patterned glass substrates were cleaned by sonication in ultrapure water, acetone, and ethanol for 20 min. Following cleaning, the substrates were dried in an oven and then subjected to UV-ozone treatment for 15 min. PVK (6 mg mL^{-1} dissolved in chlorobenzene) was spin-coated onto the ITO-patterned glass substrates at 4000 rpm for 60 s, followed by annealing at 110 °C for 10 min. Then the perovskite also was spin-coated onto the PVK at 4000 rpm for 100 s. After the anneling at 50 °C for 60 s, TPBi (40 nm), Liq (2 nm), and al (100 nm) were successively deposited using a thermal evaporation chamber (Suzhou Fangsheng FS380-S12) at a vacuum pressure of less than 4×10^{-4} Pa, with deposition rates of 2.2, 0.2, and 5 Å/s, respectively. Once the device was fabricated, it was transferred to the glove box and encapsulated with a glass cap

2.4. Characterizations

Photoluminescence (PL) spectra and photoluminescence quantum yield (PLQY) were recorded using a fluorescence spectrophotometer (Fluromax 4). The light absorption spectrum of the perovskite films was measured with a ultraviolet–visible (UV–vis) spectrometer (SPECORD S 600). Time-resolved photoluminescence (TRPL) was measured using a fluorescence spectrophotometer (HORIB-FM-2015). Current density–voltage (J-V) characteristics, electroluminescence spectra, current density-EQE curves, EQE, and operating lifetime were measured using a computer-controlled Keithley 2400 source meter, a photonic multichannel analyzer PMA-12 (Hamamatsu C10027-01), and an integrating sphere (Hamamatsu A10094). X-ray photoelectron spectroscopy (XPS) was performed using a Kratos AXIS Ultra-DLD ultrahigh vacuum surface analysis system. Field-emission scanning electron microscope (SEM) images were obtained using the ZEISS G500 and Hitachi Regulus SU8230. The trap density of states (*t*dos) and drive-level capacitance profiling (DLCP) were obtained in the dark using a Keithley 4200 digital source meter in cooperation with a Lake Shore Cryotronics probe stage. Space-charge-limited current (SCLC) curves were measured after removing the lamp. The atomic force microscopy (AFM) images were measured by a multimode V atomic force microscopy (Veeco, USA)

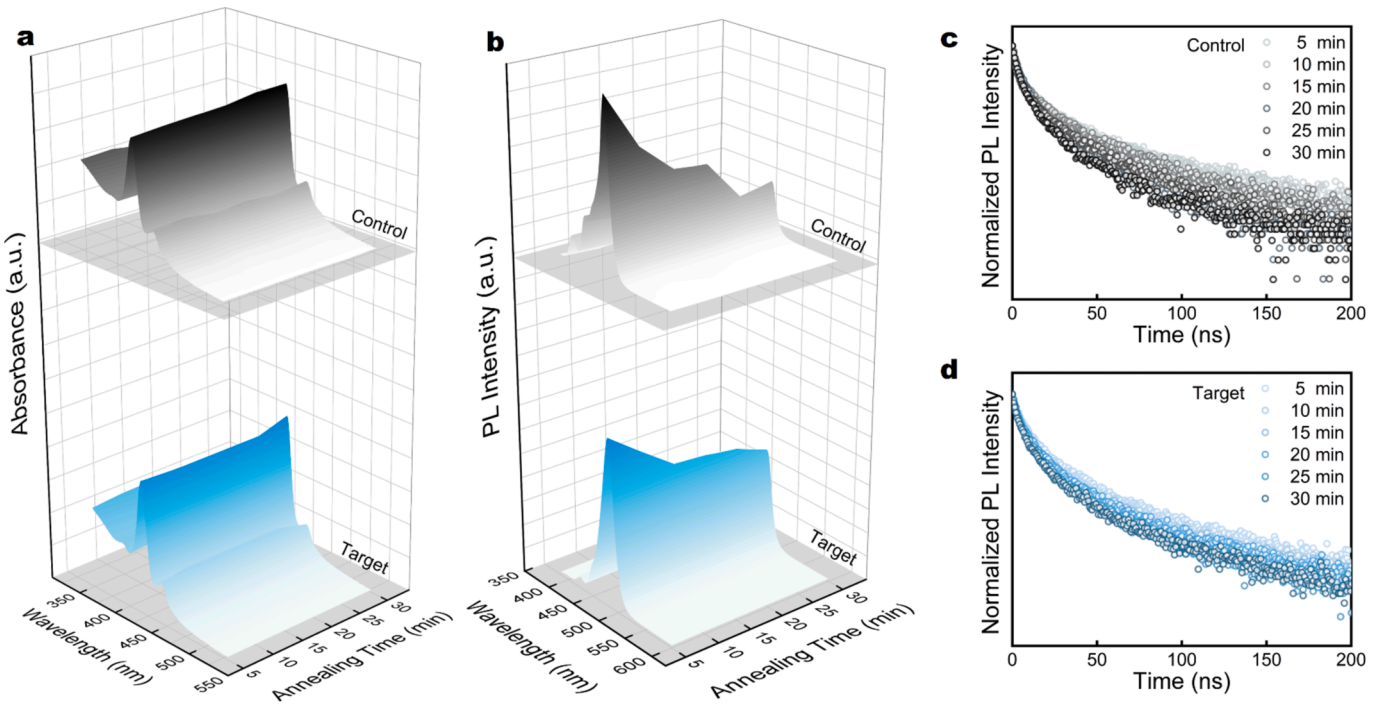


Fig. 2. (a) UV–vis spectra and (b) PL spectra of the control and target films at different annealing times at 65℃. TRPL measurement of control (c) and target (d) perovskite films at different annealing times.

3. Results and Discussion

3.1. Chlormezanone passivation mechanism

To expedite the popularity of PeLEDs in life, the prevalent approach involves using solution methods for device fabrication [27]. The hole transport layer (HTL) and EML were prepared by solution method. Initially, a layer of poly((N-vinylcarbazole) (PVK) was spin-coated onto a high-speed rotating indium tin oxide (ITO) substrate, followed by annealing. Subsequently, the perovskite film was spin-coated onto the PVK layer. This study focused on the quasi-two-dimensional perovskite structure. Typically, layered perovskite structures have the inherent capability to spontaneously form multiple quanta well structures (MQWs). Within these structures, carriers and energy can efficiently transfer from the small-n phase characterized by a wide bandgap to the large-n phase with a narrower bandgap. To stabilize this phenomenon, we introduced chlormezanone, as depicted in Fig. 1**a**, into the perovskite precursor solution. By carefully controlling the stoichiometry, we were able to precisely regulate the phase distribution, thereby increasing the proportion of the large-n phase. It is well understood that, under electrical excitation, carriers migrate from the small-n phase to the large-n phase, where, facilitated by the Coulomb force, they form electron-hole pairs, subsequently undergoing radiative recombination. However, if the small-n phase is not effectively suppressed, the presence of positive and negative ion defects may be induced by the carriers, compromising device performance [11]. Secondly, this situation will also cause very inefficient energy transfer [28]. Our research has revealed that modifying the perovskite EML with chlormezanone can effectively suppress the formation of small-n phases which is proved in the **Fig. S2**. To assess its defect passivation capacity, we employed density functional theory (DFT) to calculate the electrostatic potential (ESP) distribution of the chlormezanone molecule. In Fig. 1**b**, O atoms in S = O and C = O, show distinct electronegativity, indicative of high electron density, which serves as electron donors for coordinating with the unsaturated Pb^{2+}. And they are located on both sides of the molecule, which means that one molecule can affect multiple perovskite crystals. Fig. 1**c** illustrates the schematic diagram depicting the regulation of phase distribution and enhancement of perovskite crystallization. This enhancement is attributed to the presence of passivating functional groups (S = O, C = O) with Lewis base characteristics inherent in chlormezanone. It is well-established that the oxygen atoms within these passivating groups can offer lone pairs of electrons to neutralize unsaturated Pb^{2+} ions, thereby effectively reducing the density of trap states [29–33]. Additionally, the bonding affinity between the benzene ring and the perovskite is strengthened, leading to an enhanced film morphology characterized by increased uniformity and density [34–37]. This enhancement in surface morphology constitutes an effective approach to improve the performance of PeLEDs. For convenience of expression, using “control” to represented the original perovskite film, and “target” to represented the perovskite film modified by chlormezanone.

3.2. Thermal stability performance

At present, perovskite crystals have been prepared by crystallization in its high temperature saturated solution [38–40]. Similarly, in the process of solution preparation, the annealing temperature also has a great impact on its crystallization effect, so the following tests were carried out to evaluate the enhancement of thermal stability in EML treated by chlormezanone [41,42]. We conducted UV–vis absorption spectroscopy, PL spectroscopy, and TRPL measurements on control and chlormezanone-treated perovskite film, which were prepared under varying annealing durations. Before preparing the perovskite film, both the solution and ITO were heated to the annealing temperature to simulate the preparation process in a high temperature environment, such as the cooling crystallization method to prepare the perovskite crystal. The characteristic peaks observed at 390 nm, 420 nm, and 455 nm are attributed to the small-n phases, corresponding to n = 1, 2, and 3, respectively [43]. Moreover, the presence of a characteristic peak at 486 nm indicates the structural features of 3D perovskite crystal [44,45]. Notably, with increasing annealing duration, the magnitude of change in the small-n phase of the target film remained minimal, while a increase was observed in the control, particularly in the n = 2 phase (refer to Fig. 2**a**). Additionally, when comparing the UV–vis absorption spectra of

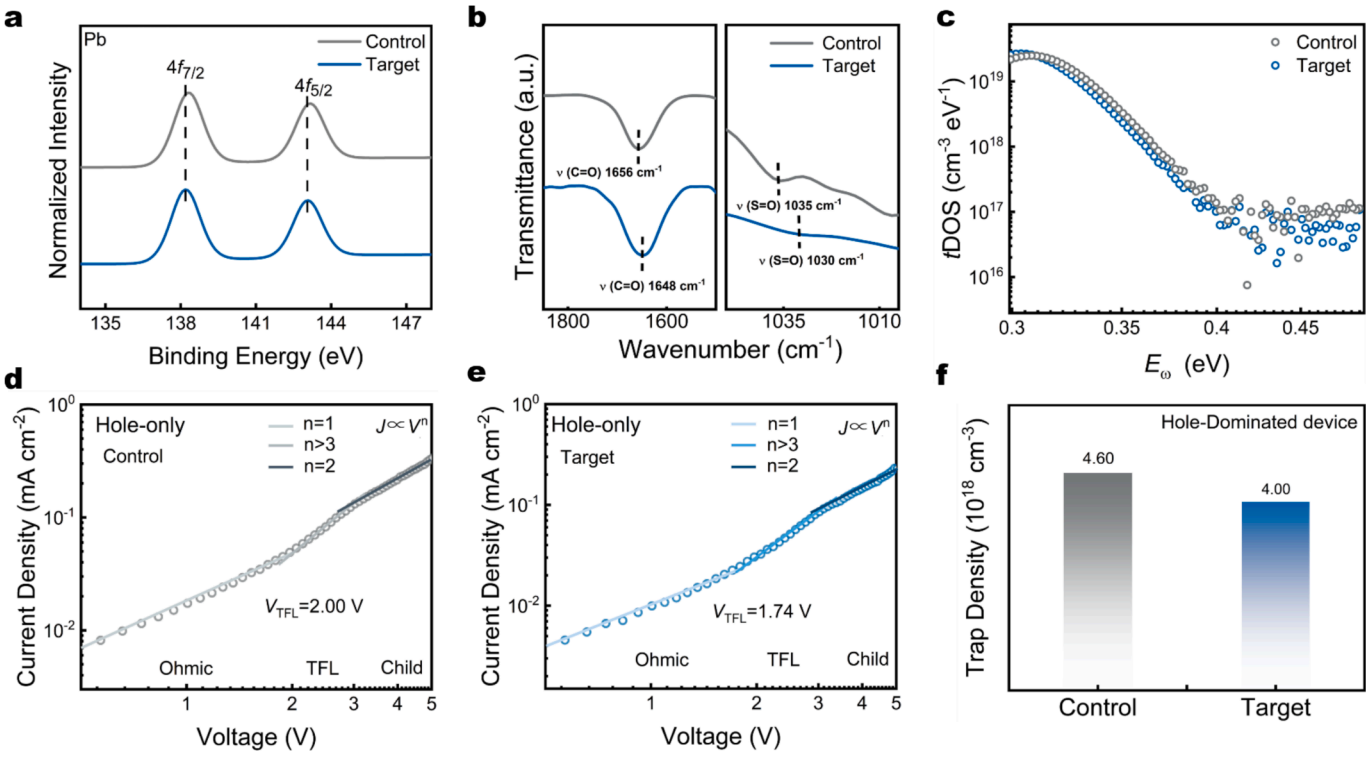


Fig. 3. (a) High-resolution XPS spectra of the control and target perovskite films showing the Pb 4*f* core levels. (b) FTIR spectra of the chlormezanone molecule and $PbBr_2$ with chlormezanone. (c) The *t*DOS curves of the control and target devices. (d) The SCLC curves of the control device. (e) The SCLC curves of the target device. (f) The trap density of the control and target devices calculated by DLCP.

perovskite films annealed for 30 min (**Fig. S3**), a significant difference was observed in the n = 1 phase between the control and target perovskite films. These findings suggested that this method can delay the increase of the small-n phase, thereby improving the lifetime and performance of the EML. Subsequently, we analyzed the PL spectra data to further validate the reliability of this approach. As depicted in Fig. 2**b**, the intensity of the peak at 488 nm in the control gradually diminished with prolonged annealing, while the target sample exhibited a slower decay rate. A comparison of the PL spectra of perovskite films annealed for 30 min revealed that the target perovskite films maintain a stable state, while the control films exhibited more pronounced degradation (**Fig. S4**). These observations highlighted the ability of chlormezanone to suppress small-n phase formation and enhance the thermal stability of the EML. Furthermore, TRPL measurements were conducted to investigate the recombination dynamics of excited charge carriers in systems subjected to different annealing durations [46]. The TRPL decay curve can be modeled in terms of a three-exponential function:

$$I(t) = A_1 exp(-t/\tau_1) + A_2 exp(-t/\tau_2) + A_3 exp(-t/\tau_3) \quad (1)$$

where I is the normalized PL intensity, A_1, A_2 and A_3 are the ratios of the three decays, and τ_1, τ_2 and τ_3 represent the fast, medium and slow decay lifetimes, respectively. The average lifetime of the perovskite film is given by

$$\tau_{ave} = (A_1\tau_1 + A_2\tau_2 + A_3\tau_3)/(A_1 + A_2 + A_3) \quad (2)$$

and the results in **Table S1**. A comparison of Fig. 2**c and 2d** revealed that after the same duration (200 ns), the normalized PL intensity of the target perovskite showed a smaller decrement, with closer data overlap. This finding indicated that this method effectively reduced device degradation at high temperatures and extended device lifespan. Additionally, we compared the TRPL lifetimes of perovskite films annealed for 30 min and found that the half-life of the control sample was shorter than that of the target sample (**Fig. S5**), further supporting the aforementioned conclusion.

3.3. Reason of defects reduction

To further elucidate the interaction between chlormezanone and perovskite, we performed high-resolution XPS analysis to investigate the chemical states of Pb $4f_{5/2}$ and $4f_{7/2}$. As shown in Fig. 3**a**, compared to the control film, the core levels of Pb $4f_{5/2}$ and $4f_{7/2}$ exhibited a noticeable shift to lower binding energy in the chlormezanone-treated film. This reduction in binding energy can be attributed to the empty 6p orbital of Pb^{2+} accepting lone pair electrons from the oxygen atom of the C = O and S = O groups, providing evidence for the coordination between chlormezanone and unsaturated Pb^{2+} [47–50]. Next, Fourier-transform infrared spectroscopy (FTIR) was conducted to analyze the passivation effect of chlormezanone. Fig. 3**b** presented the FTIR spectra of chlormezanone and its mixture with $PbBr_2$. Upon the addition of $PbBr_2$, the stretching vibration peaks of the S = O and C = O functional groups in chlormezanone shifted to lower wavenumbers (from 1035 and 1656 cm^{-1} to 1030 and 1648 cm^{-1}, respectively), indicating coordination between the oxygen atoms in the S = O and C = O groups of chlormezanone and Pb^{2+} [51]. The XPS and FTIR analyses collectively elucidated the defect passivation effect of chlormezanone on perovskite films. To further illustrate the defect passivation function of this molecule, we plotted the *t*DOS as a function of energy space in Fig. 3**c**. The data indicated that the target device had a significantly lower defect density in the shallow-level energy space. Subsequently, we performed SCLC characterization to investigate the impact of chlormezanone on trap states density and carrier mobility in more detail. The *J-V* curves obtained using the SCLC method were analyzed in three regions: the linear ohmic region, the defect-filled region, and the current region. Hole-only devices were fabricated for both the control and target samples to measure the defect-filled voltage (V_{TFL}). Analysis of Fig. 3**d and 3e** revealed that the V_{TFL} for the control device was 2.00 V, whereas the V_{TFL} for the target device was 1.74 V. Additionally, the passivation effect

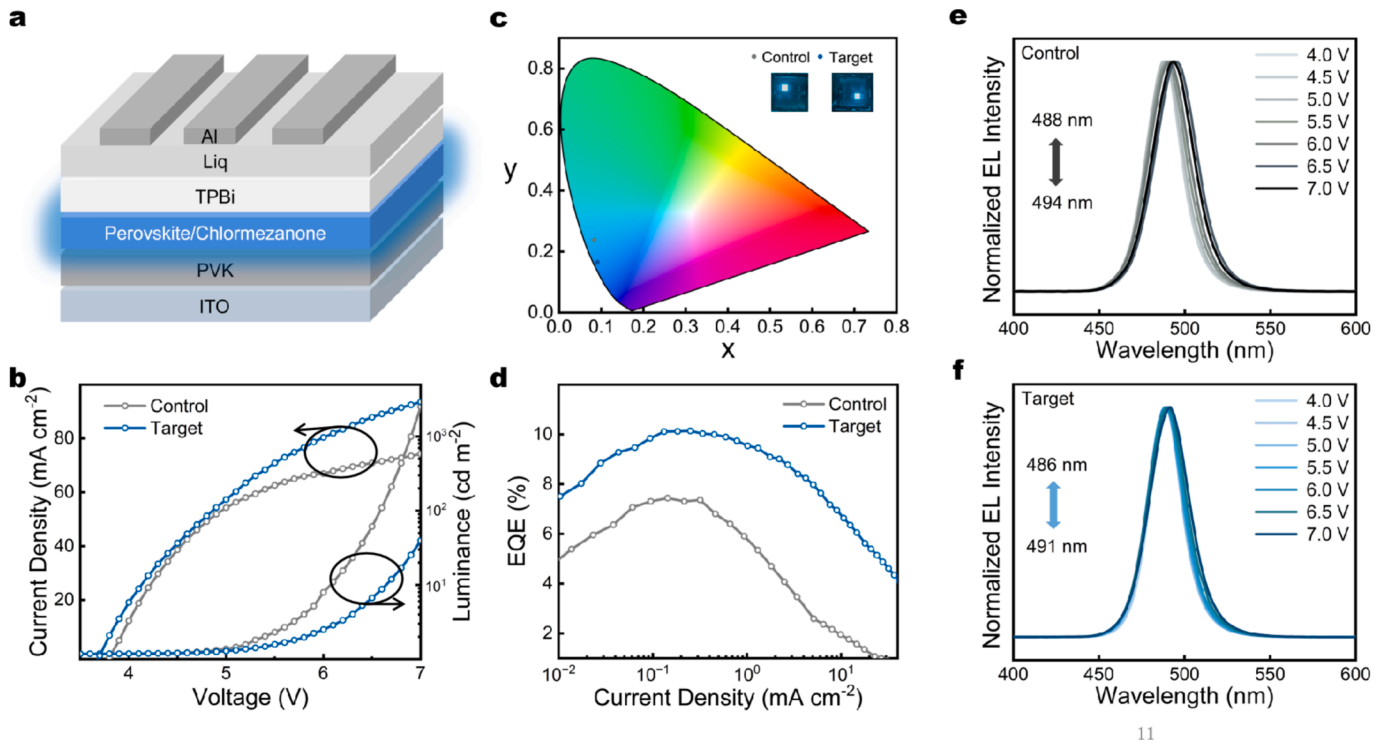


Fig. 4. (a) The device structure of PeLEDs. (b) Current density–voltage-luminance curves, (c) CIE coordinate and (d) current density-EQE curves of control and target devices. Normalized EL spectra of control (e) and target (f) PeLEDs under a series of different bias voltages.

of chlormezanone was demonstrated using DLCP, as shown in Fig. 3**f**, which illustrates the reduction in defect density in the target device. Applying the formula:

$$N_{\text{trap}} = 2V_{\text{TFL}}\frac{\varepsilon_r\varepsilon_0}{qL^2} \tag{3}$$

where ε_0, ε_r, q and L represent the relative permittivity of the perovskite, the vacuum permittivity, the unit charge, and thickness of the perovskite layer, respectively, and V_{TFL} was the trap-filling limit voltage [52]. The defect density of the control film was calculated to be 4.60×10^{18} cm^{-3}, whereas the defect density of the target device was determined to be 4.00×10^{18} cm^{-3}. This analysis corroborated the effectiveness of the method.

The PLQY of perovskite films treated with chlormezanone (71.8 %) was approximately 1.4 times higher than that of the untreated perovskite films (49.7 %), indicating that chlormezanone treatment enhances PLQY and promotes carrier recombination (**Fig. S6**). According to.

$$\text{PLQY} = k_r/(k_r + k_{nr}) \tag{4}$$

and

$$\tau_{ave} = (k_r + k_{nr})^{-1} \tag{5}$$

we can get the radiative recombination rate (k_r) and the non-radiative recombination rate (k_{nr}). In addition, there is a competitive relationship between radiative recombination and non-radiative recombination [53]. As shown in **Fig. S7**, the radiation recombination rate of the treated perovskite film ($16.28 \times 10^7 s^{-1}$) was higher than that of the original perovskite film ($15.78 \times 10^7 s^{-1}$). The non-radiative recombination rate ($6,39 \times 10^7 s^{-1}$) was lower than that of the original perovskite film ($15.97 \times 10^7 s^{-1}$), indicating that chlormezanone treatment could effectively promote radiative recombination and improved the photoluminescence efficiency [54,55].

Furthermore, top-view SEM and AFM were employed to assess the quality of perovskite films. The images of AFM of the control and the target perovskite film were displayed in **Fig. S8(a) and (c)**, the mean surface roughness (Ra) value of the perovskite film decreased from 5.87 to 4.03 nm, this additionally underscored the capacity of chlormezanone to promote the growth of perovskite film. The images of SEM of the control and the target films in **Fig. S8(b) and (d)** also supported the improvements in the crystallization of the perovskite layer. The reducing of the density of defects can decrease the move of ions, which means the reduce of the leakage current [56–58]. Better film morphology reflects the less defects so that the additive can reduce the leakage current of device.

3.4. Electroluminescence performance of PeLEDs

In order to test the electrical properties of the perovskite layer, we produced PeLEDs with p-i-n structure, as shown in Fig. 4**a**. As perovskite displays and lighting will continue to be powered by electricity in the future, we conducted electroluminescence (EL) tests to evaluate the EL performance. For additives, the common concern is that the addition of organic additives will cause an increase in the resistance value of the device and a decrease in current density [59]. Comparing the original device and the chlormezanone treated device in Fig. 4**b**, current density of the target device was lower than control device. But their luminance is the opposite. Low concentration of chlormezanone can still effectively improve device performance and reduce adverse effects through the passivation functional groups distributed on both sides [25]. After detection, it is found that the light emitted by the target device (486 nm) is blue shifted by 2 nm compared to the light emitted by the control device (488 nm). In the CEI diagram, the coordinate of the light of the target device is (0.09, 0.16) and the coordinate of the light of the control device is (0.08, 0.23) shown in Fig. 4**c**. The reason for the blue shift of luminous peak is that the additive chlormezanone contains chloride ions, and the increase of perovskite chloride ion concentration will cause the blue shift of luminous peak [60,61]. The important thing is that this method indeed improves EQE, reaching 10.14 %. The repeatability of the this method is proved by the 60 devices in **Fig. S9**. The average EQE of target PeLEDs is 8.57 % and for control devices, it is 6.00 %. In

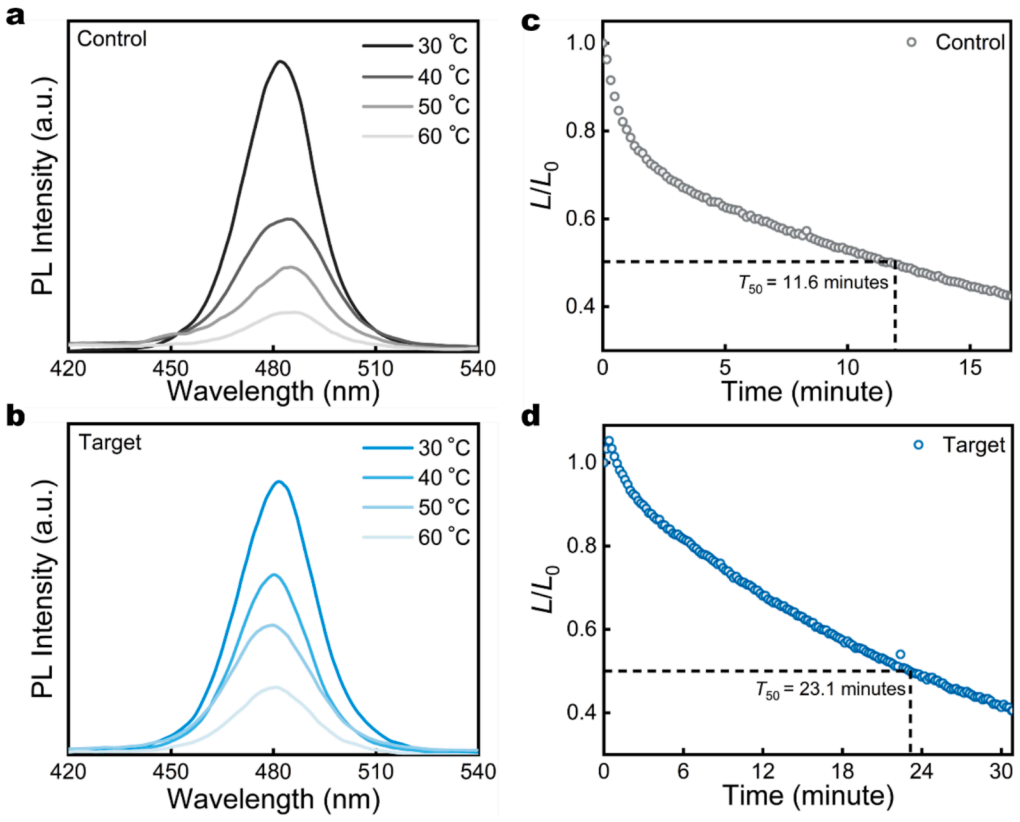


Fig. 5. PL spectra of the control (a) and target (b) films processed in a series of different temperature conditions after 10 min. T_{50} lifetime measurements of control (c) and target (d) devices under constant work current density of 1 mA cm^{-2}.

addition, when the applied voltage was increased from 4 V to 7 V, the peak emission wavelength of the control device red-shifted by 6 nm, and that of the target device only red-shifted by 5 nm. This suggests that the target PeLED was more stable in terms of emission wavelength under varying voltages, which is advantageous for practical applications (Fig. 4**e and 4f**).

3.5. *Extension of electroluminescence lifetime*

LED will inevitably heat in the case of power, in order to ensure the minimum life of it, in addition to the structure to make it easier to heat dissipation, improve its own thermal stability is also particularly important. The two perovskite films were placed at 30, 40, 50 and 60℃ for ten minutes to know the degree of film decomposition. In Fig. 5**a and 5b**, the target film obviously had higher PL intensity than the control film, which means better thermal stability. Then its electroluminescent lifetime was tested. Under a constant current density of 1 mA cm^{-2}, the T_{50} lifetime (the time it takes for the brightness to decrease to half of its initial value) of the target device was 23.1 min, nearly twice as long as that of the control device (Fig. 5**b and 5d**). This provided further evidence of the enhancement in device lifetime and stability achieved with this approach.

4. Conclusion

In summary, we utilized chlormezanone, an organic molecule featuring two passivating groups (one C = O double bond and two S = O double bonds) to modify trap states and regulate phase distribution in sky-blue PeLEDs. Our findings indicated that this approach effectively delays the formation of small-n phases and mitigated the decomposition of the perovskite layer under high-temperature conditions, thereby extending the device's operational lifetime. This work offered a strategy to enhance the thermal stability and lifetime of sky-blue PeLEDs, providing a viable solution for their application in high-temperature environments or under prolonged operating conditions. At the same time, it also inspired the strategy of ensuring crystal stability during the crystallization and growth of perovskite in solution.

CRediT authorship contribution statement

Shao-Qi Wang: Writing – original draft. **Wei Yang:** Investigation. **Yu Xia:** Visualization. **Bin Wang:** Methodology. **Nan Li:** Resources. **Lei Huang:** Resources. **Xin Chen:** Methodology. **Yu-Han Li:** Visualization. **Jing Chen:** Supervision. **Chun-Hao Chen:** Visualization. **Zhao-Kui Wang:** Funding acquisition.

Declaration of competing interest

The authors declare that they have no known competing financial interests or personal relationships that could have appeared to influence the work reported in this paper.

Acknowledgements

The authors acknowledged financial support from the National Natural Science Foundation of China (No. 52273189), the Natural Science Foundation of Jiangsu Province (Nos. BZ2023052, BE20220262), and Suzhou science and technology plan project (Nos. N321461821 and ST202212). This work is supported by Suzhou Key Laboratory of Functional Nano & Soft Materials, Collaborative Innovation Center of Suzhou Nano Science & Technology, the 111 Project, Joint International Research Laboratory of Carbon-Based Functional Materials and Devices, and Soochow University Tang Scholar.

Appendix A. Supplementary data

Supplementary data to this article can be found online at https://doi.org/10.1016/j.cej.2025.159796.

Data availability

Data will be made available on request.

References

[1] J. Zhang, L. Wang, X. Zhang, G. Xie, G. Jia, J. Zhang, X. Yang, Blue light-emitting diodes based on halide perovskites: Recent advances and strategies, Mater. Today 51 (2021) 222–246, https://doi.org/10.1016/j.mattod.2021.10.023.

[2] Z.K. Tan, R.S. Moghaddam, M.L. Lai, P. Docampo, R. Higler, F. Deschler, M. Price, A. Sadhanala, L.M. Pazos, D. Credgington, F. Hanusch, T. Bein, H.J. Snaith, R. H. Friend, Bright light-emitting diodes based on organometal halide perovskite, Nat. Nanotechnol 9 (2014) 687–692.

[3] K. Lin, J. Xing, L.N. Quan, F.P.G. de Arquer, X. Gong, J. Lu, L. Xie, W. Zhao, D. Zhang, C. Yan, W. Li, X. Liu, Y. Lu, J. Kirman, E.H. Sargent, Q. Xiong, Z. Wei, Perovskite light-emitting diodes with external quantum efficiency exceeding 20 per cent, Nature 562 (2018) 245–248.

[4] X. Liang, Z. Liu, J. Zhang, H. Chen, Q. Gu, W. Zhang, C. Shen, Z. Xiao, Y. Wang, J. Liao, X. Wen, J. Xie, L. Yao, W. Cai, Y. Mo, J. Qing, S.J. Su, L. Hou, Promoting Energy Transfer Between Quasi-2D Perovskite Layers Toward Highly Efficient Red Light-Emitting Diodes, Small 18 (2022) e2204638.

[5] Y.-H. Li, Y.-H. Lou, Y.-H. Zhou, Y. Xia, B. Wang, Z.-K. Wang, Review on the promising roles of alkali metals toward highly efficient perovskite light-emitting diodes, J. Mater. Chem. C 11 (2023) 2011–2025. https://pubs.rsc.org/en/content/articlelanding/2023/tc/d2tc04629f.

[6] Y. Gao, Q. Cai, Y. He, D. Zhang, Q. Cao, M. Zhu, Z. Ma, B. Zhao, H. He, D. Di, Z. Ye, X. Dai, Highly efficient blue light-emitting diodes based on mixed-halide perovskites with reduced chlorine defects, Sci. Adv 10 (2024) eado5645, https://doi.org/10.1126/sciadv.ado5645.

[7] S.C. Feng, Y. Shen, X.M. Hu, Z.H. Su, K. Zhang, B.F. Wang, L.X. Cao, F.M. Xie, H. Z. Li, X. Gao, J.X. Tang, Y.Q. Li, Efficient and Stable Red Perovskite Light-Emitting Diodes via Thermodynamic Crystallization Control, Adv. Mater (2024) e2410255.

[8] S.Q. Sun, J.W. Tai, W. He, Y.J. Yu, Z.Q. Feng, Q. Sun, K.N. Tong, K. Shi, B.C. Liu, M. Zhu, G. Wei, J. Fan, Y.M. Xie, L.S. Liao, M.K. Fung, Enhancing Light Outcoupling Efficiency via Anisotropic Low Refractive Index Electron Transporting Materials for Efficient Perovskite Light-Emitting Diodes, Adv. Mater (2024) e2400421.

[9] Y.H. Li, Y. Xia, Z. Zhang, B. Wang, R.J. Jin, C.H. Chen, J. Chen, K.L. Wang, G. Xing, Z.K. Wang, L.S. Liao, In Situ Hydrolysis of Phosphate Enabling Sky-Blue Perovskite Light-Emitting Diode with EQE Approaching 16.32, ACS Nano 18 (2024) 6513–6522.

[10] X. Yang, L. Ma, M. Yu, H.H. Chen, Y. Ji, A. Hu, Q. Zhong, X. Jia, Y. Wang, Y. Zhang, R. Zhu, X. Wang, C. Lu, Focus on perovskite emitters in blue light-emitting diodes, Light Sci. Appl 12 (2023) 177.

[11] S. Bera, A. Saha, S. Mondal, A. Biswas, S. Mallick, R. Chatterjee, S. Roy, Review of defect engineering in perovskites for photovoltaic application, Mater. Adv 3 (2022) 5234–5247. https://www.sciencedirect.com/org/science/article/pii/S2633540923014251.

[12] N. Li, Y. Xia, Y.-H. Lou, Y.-H. Li, R.-J. Jin, X.-Y. He, C.-H. Chen, J. Chen, K.-L. Wang, Z.-K. Wang, Dual-functional self-assembled molecule enabling high-performance deep-blue perovskite light-emitting diodes, Adv. Funct. Mater (2024) 2411227, https://doi.org/10.1002/adfm.202411227.

[13] Y. Xia, Y.-H. Li, Z.-K. Wang, L.-S. Liao, Domain distribution management of quasi-2D perovskites toward high-performance blue light-emitting diodes, Adv. Funct. Mater 33 (2023) 2303423, https://doi.org/10.1002/adfm.202303423.

[14] Y. Xia, B. Song, Z. Zhang, K.L. Wang, Y.H. Li, N. Li, C.H. Chen, J. Chen, G. Xing, Z. K. Wang, Vertically concentrated quantum wells enabling highly efficient deep-blue perovskite light-emitting diodes, Angew. Chem. Int. Ed 63 (2024) e202403739.

[15] Y.-H. Li, Y. Xia, C.-H. Chen, R.-J. Jin, A. Nar, J. Chen, N. Li, K.-L. Wang, I. Yavuz, Z.-K. Wang, Surficial homogenic effect enables highly stable deep-blue perovskite light-emitting diodes, Angew. Chem. Int. Ed (2024) e202412915, https://doi.org/10.1002/anie.202412915.

[16] B. Wang, Y.-H. Lou, Y. Xia, F. Hu, Y.-H. Li, K.-L. Wang, J. Chen, C.-H. Chen, Z.-H. Su, X.-Y. Gao, Z.-K. Wang, Chemical reaction modulated low-dimensional phase toward highly efficient sky-blue perovskite light-emitting diodes, Angew. Chem. Int. Ed 63 (2024) e202406140, https://doi.org/10.1002/anie.202406140.

[17] X. Yang, X. Zhang, J. Deng, Z. Chu, Q. Jiang, J. Meng, P. Wang, L. Zhang, Z. Yin, J. You, Efficient green light-emitting diodes based on quasi-two-dimensional composition and phase engineered perovskite with surface passivation, Nat. Commun 9 (2018) 570.

[18] Y. Zhou, J. Chen, O.M. Bakr, H.-T. Sun, Metal-doped lead halide perovskites: synthesis, properties, and optoelectronic applications, Chem. Mater 30 (2018) 6589–6613. https://pubs.acs.org/doi/10.1021/acs.chemmater.8b02989.

[19] Y. Xia, Y.H. Lou, Y.H. Zhou, Y.R. Shi, K.L. Wang, L. Cai, C.H. Chen, F. Hu, Z. K. Wang, L.S. Liao, Reduced confinement effect by isocyanate passivation for efficient sky-blue perovskite light-emitting diodes, Adv. Funct. Mater 32 (2022), https://doi.org/10.1002/adfm.202208538.

[20] D. Ma, K. Lin, Y. Dong, H. Choubisa, A.H. Proppe, D. Wu, Y.K. Wang, B. Chen, P. Li, J.Z. Fan, F. Yuan, A. Johnston, Y. Liu, Y. Kang, Z.H. Lu, Z. Wei, E.H. Sargent, Distribution control enables efficient reduced-dimensional perovskite LEDs, Nature 599 (2021) 594–598.

[21] L. Na Quan, D. Ma, Y. Zhao, O. Voznyy, H. Yuan, E. Bladt, J. Pan, F.P. Garcia de Arquer, R. Sabatini, Z. Piontkowski, A.H. Emwas, P. Todorovic, R. Quintero-Bermudez, G. Walters, J.Z. Fan, M. Liu, H. Tan, M.I. Saidaminov, L. Gao, Y. Li, D. H. Anjum, N. Wei, J. Tang, D.W. McCamant, M.B.J. Roeffaers, S. Bals, J. Hofkens, O.M. Bakr, Z.H. Lu, E.H. Sargent, Edge stabilization in reduced-dimensional perovskites, Nat. Commun 11 (2020) 170.

[22] W. Xu, Q. Hu, S. Bai, C. Bao, Y. Miao, Z. Yuan, T. Borzda, A.J. Barker, E. Tyukalova, Z. Hu, M. Kawecki, H. Wang, Z. Yan, X. Liu, X. Shi, K. Uvdal, M. Fahlman, W. Zhang, M. Duchamp, J.-M. Liu, A. Petrozza, J. Wang, L.-M. Liu, W. Huang, F. Gao, Rational molecular passivation for high-performance perovskite light-emitting diodes, Nat. Photonics 13 (2019) 418–424. https://www.nature.com/articles/s41566-019-0390-x.

[23] H. Wang, X. Zhang, Q. Wu, F. Cao, D. Yang, Y. Shang, Z. Ning, W. Zhang, W. Zheng, Y. Yan, S.V. Kershaw, L. Zhang, A.L. Rogach, X. Yang, Trifluoroacetate induced small-grained CsPbBr(3) perovskite films result in efficient and stable light-emitting devices, Nat. Commun 10 (2019) 665.

[24] H. Li, C. Li, T. Yin, Q. Yu, S. Jin, H. He, Q. Shen, M. Huang, P. Zhong, N. Cui, C. Shou, Undercoordinated Pb2+ defects passivation via tetramethoxysilane-modified for efficient and stable perovskite solar cells, Org. Electron. 99 (2021) 106332. https://www.sciencedirect.com/science/article/abs/pii/S1566119921002688.

[25] S.Q. Sun, Q. Sun, Y.J. Ji, Y.L. Xu, W. He, M. Zhu, J.G. Zhou, Y.J. Yu, D.D. Feng, Y. M. Xie, Y.Y. Li, M.K. Fung, Multidentate molecule anchoring halide perovskite surface and regulating crystallization kinetics toward efficient light-emitting diodes, Small 19 (2023) e2205336.

[26] Z. Yu, X. Shen, X. Fan, Y.-K. Jung, W.H. Jeong, A. Dasgupta, M. Kober-Czerny, P. Caprioglio, S.H. Park, H. Choi, H.J. Snaith, S.D. Stranks, B.R. Lee, Hydrogen bond-assisted dual passivation for blue perovskite light-emitting diodes, ACS Energy Lett 8 (2023) 4296–4303. https://pubs.acs.org/doi/10.1021/acsenergylett.3c01323.

[27] L. Chao, T. Niu, W. Gao, C. Ran, L. Song, Y. Chen, W. Huang, Solvent engineering of the precursor solution toward large-area production of perovskite solar cells, Adv. Mater 33 (2021) 2005410.

[28] L. Kong, X. Zhang, Y. Li, H. Wang, Y. Jiang, S. Wang, M. You, C. Zhang, T. Zhang, S. V. Kershaw, W. Zheng, Y. Yang, Q. Lin, M. Yuan, A.L. Rogach, X. Yang, Smoothing the energy transfer pathway in quasi-2D perovskite films using methanesulfonate leads to highly efficient light-emitting devices, Nat. Commun 12 (2021) 1246.

[29] Y. Sun, L. Ge, L. Dai, C. Cho, J. Ferrer Orri, K. Ji, S.J. Zelewski, Y. Liu, A. J. Mirabelli, Y. Zhang, J.Y. Huang, Y. Wang, K. Gong, M.C. Lai, L. Zhang, D. Yang, J. Lin, E.M. Tennyson, C. Ducati, S.D. Stranks, L.S. Cui, N.C. Greenham, Bright and stable perovskite light-emitting diodes in the near-infrared range, Nature 615 (2023) 830–835.

[30] S. Lee, J. Kim, H. Kim, C. Kim, S. Kim, C. Kim, H. Lee, B. Choi, C. Muthu, T. Kim, J. Lee, S. Lee, H. Ihee, J.Y. Lee, Brightening deep-blue perovskite light-emitting diodes: A path to Rec. 2020, in: Sci Adv, 10, 2024.

[31] B. Chen, H. Liu, J. Yang, M. Ahmadi, Q. Chen, N. Yin, S. Zhang, M. Xiao, H. Zhang, L. Xu, P. Chen, Coordination of thermally activated delayed fluorescent molecules for efficient and stable perovskite light-emitting diodes, Adv. Funct. Mater (2024) 2402522, https://doi.org/10.1002/adfm.202402522.

[32] C. Zhao, Y. Li, W. Ye, X. Shen, Z. Wen, X. Yuan, Y. Cao, C. Ma, Ligand-free CsPbBr3 perovskite quantum dots in silica-aerogel composites with enhanced stability for w-LED and display by substituting Pb2+ with Pr3+ or Gd3+ ions, Adv. Opt. Mater 10 (2022) 202102200, https://doi.org/10.1002/adom.202102200.

[33] L. Wen, Y. Rao, M. Zhu, R. Li, J. Zhan, L. Zhang, L. Wang, M. Li, S. Pang, Z. Zhou, Reducing Defects Density and Enhancing Hole Extraction for Efficient Perovskite Solar Cells Enabled by pi-Pb(2+) Interactions, Angew Chem. Int. Ed. Engl 60 (2021) 17356–17361.

[34] H. Lee, J.W. Jeong, M.G. So, G.Y. Jung, C.L. Lee, Design of chemically stable organic perovskite quantum dots for micropatterned light-emitting diodes through kinetic control of a cross-linkable ligand system, Adv. Mater 33 (2021) e2007855.

[35] C. Gao, R. Li, Y. Li, R. Wang, M. Wang, Z. Gan, L. Bai, Y. Liu, K. Zhao, S.F. Liu, Y. Cheng, W. Huang, Direct-Indirect Transition of Pressurized Two-Dimensional Halide Perovskite: Role of Benzene Ring Stack Ordering, J. Phys. Chem. Lett 10 (2019) 5687–5693.

[36] P. Lu, T. Li, M. Lu, C. Ruan, S. Sun, Z. Wu, Y. Zhong, F. Zhang, Y. Gao, Y. Huang, Y. Wang, J. Hu, F. Yan, Y. Zhang, Enrichment of anchoring sites by introducing supramolecular halogen bonds for the efficient perovskite nanocrystal LEDs, Light Sci Appl 12 (2023) 215.

[37] J. Zhang, B. Cai, X. Zhou, F. Yuan, C. Yin, H. Wang, H. Chen, X. Ji, X. Liang, C. Shen, Y. Wang, Z. Ma, J. Qing, Z. Shi, Z. Hu, L. Hou, H. Zeng, S. Bai, F. Gao, Ligand-induced cation-pi interactions enable high-efficiency, bright, and spectrally stable rec. 2020 pure-red perovskite light-emitting diodes, Adv. Mater 35 (2023) e2303938. https://www.ncbi.nlm.nih.gov/pubmed/37464982.

[38] Y. Chen, X. Yang, X. Fan, A. Kang, X. Kong, G. Chen, C. Zhong, Y. Lu, Y. Fan, X. Hou, T. Wu, Z. Chen, S. Wang, Y. Lin, Electrohydrodynamic inkjet printing of three-dimensional perovskite nanocrystal arrays for full-color micro-LED displays, ACS Appl. Mater. Interfaces 16 (2024) 24908–24919, https://doi.org/10.1021/acsami.4c02594.

[39] X. Fan, X. Yang, X. Kong, T. Zhang, S. Wang, Y. Lin, Z. Chen, Recent progresses on perovskite quantum dots patterning techniques for color conversion layer in micro-LED displays, Next Nanotechnology 5 (2024) 100045, https://doi.org/10.1016/j.nxnano.2024.100045.

[40] S.-S. Rong, M.B. Faheem, Y.-B. Li, Perovskite single crystals: synthesis, properties, and applications, J. Electron. Sci. Technol 19 (2021) 100081. https://www.sciencedirect.com/science/article/pii/S1674862X21000021.
[41] D. Zheng, F. Raffin, P. Volovitch, T. Pauporte, Control of perovskite film crystallization and growth direction to target homogeneous monolithic structures, Nat. Commun 13 (2022) 6655.
[42] H. Zhou, K. Cai, S. Yu, Z. Wang, Z. Xiong, Z. Chu, X. Chu, Q. Jiang, J. You, Efficient and stable perovskite mini-module via high-quality homogeneous perovskite crystallization and improved interconnect, Nat. Commun 15 (2024) 6679.
[43] J. Xing, Y. Zhao, M. Askerka, L.N. Quan, X. Gong, W. Zhao, J. Zhao, H. Tan, G. Long, L. Gao, Z. Yang, O. Voznyy, J. Tang, Z.H. Lu, Q. Xiong, E.H. Sargent, Color-stable highly luminescent sky-blue perovskite light-emitting diodes, Nat. Commun 9 (2018) 3541.
[44] W. Yang, C.-H. Gao, Y. Xia, B. Wang, K.-L. Wang, Y.-H. Lou, Z.-K. Wang, Enhancing energy channel and carriers recycling in sky-blue perovskite light-emitting diodes via a fluorescent fortifier, Appl. Phys. Lett 123 (2023) 153520, https://doi.org/10.1063/5.0172757.
[45] P. Pang, G. Jin, C. Liang, B. Wang, W. Xiang, D. Zhang, J. Xu, W. Hong, Z. Xiao, L. Wang, G. Xing, J. Chen, D. Ma, Rearranging low-dimensional phase distribution of quasi-2D perovskites for efficient sky-blue perovskite light-emitting diodes, ACS Nano 14 (2020) 11420–11430.
[46] E.V. Pean, S. Dimitrov, C.S. De Castro, M.L. Davies, Interpreting time-resolved photoluminescence of perovskite materials, Phys. Chem. Chem. Phys 22 (2020) 28345–28358.
[47] Y. Miao, G. Sathiyan, H. Wang, Y. Tian, C. Chen, X. Ding, M. Zhai, X. Yang, M. Cheng, Construction of efficient perovskite solar cell through small-molecule synergistically assisted surface defect passivation and fluorescence resonance energy transfer, Chem. Eng. J 426 (2021) 131358, https://doi.org/10.1016/j.cej.2021.131358.
[48] Q. Zhou, J. Qiu, Y. Wang, M. Yu, J. Liu, X. Zhang, Multifunctional chemical bridge and defect passivation for highly efficient inverted perovskite solar cells, ACS Energy Lett (2021) 1596–1606. https://pubs.acs.org/doi/10.1021/acsenergylett.1c00291.
[49] X. Ding, H. Wang, C. Chen, H. Li, Y. Tian, Q. Li, C. Wu, L. Ding, X. Yang, M. Cheng, Passivation functionalized phenothiazine-based hole transport material for highly efficient perovskite solar cell with efficiency exceeding 22%, Chem. Eng. J 410 (2021) 128328. https://www.sciencedirect.com/science/article/abs/pii/S1385894720344405.
[50] S. Yang, S. Chen, E. Mosconi, Y. Fang, X. Xiao, C. Wang, Y. Zhou, Z. Yu, J. Zhao, Y. Gao, F. De Angelis, J. Huang, Stabilizing halide perovskite surfaces for solar cell operation with wide-bandgap lead oxysalts, Science 365 (2019) 473–478.
[51] M. Wang, F. Cao, M. Wang, K. Deng, L. Li, Intermediate-adduct-assisted growth of stable CsPbI(2) Br inorganic perovskite films for high-efficiency semitransparent solar cells, Adv Mater 33 (2021) e2006745.
[52] L. Huang, K.-L. Wang, R.-J. Jin, J. Chen, C.-H. Chen, Y. Xia, Y.-H. Lou, Z.-K. Wang, Reshaped buried interface by comprehensive passivation for highly efficient perovskite photovoltaics, Chem. Eng. J 488 (2024) 150815.
[53] Z. Chu, Y. Zhao, F. Ma, C.X. Zhang, H. Deng, F. Gao, Q. Ye, J. Meng, Z. Yin, X. Zhang, J. You, Large cation ethylammonium incorporated perovskite for efficient and spectra stable blue light-emitting diodes, Nat. Commun 11 (2020) 4165.
[54] Y.H. Kim, H. Cho, T.W. Lee, Metal halide perovskite light emitters, Proc Natl Acad Sci U S A 113 (2016) 11694–11702.
[55] J. Tao, C. Sun, H. Zhang, T. Wei, D. Xu, J. Han, C. Fan, Z.H. Zhang, W. Bi, Perovskite energy funnels for efficient white emission, J Colloid Interface Sci 608 (2022) 1202–1211.
[56] J. Chmeliov, K. Elkhouly, R. Gegevičius, L. Jonušis, A. Devižis, A. Gelžinis, M. Franckevičius, I. Goldberg, J. Hofkens, P. Heremans, W. Qiu, V. Gulbinas, Ion motion determines multiphase performance dynamics of perovskite LEDs, Adv. Opt. Mater 9 (2021) 2101560, https://doi.org/10.1002/adom.202101560.
[57] H. Kim, J.S. Kim, J.-M. Heo, M. Pei, I.-H. Park, Z. Liu, H.J. Yun, M.-H. Park, S.-H. Jeong, Y.-H. Kim, J.-W. Park, E. Oveisi, S. Nagane, A. Sadhanala, L. Zhang, J. J. Kweon, S.K. Lee, H. Yang, H.M. Jang, R.H. Friend, K.P. Loh, M.K. Nazeeruddin, N.-G. Park, T.-W. Lee, Proton-transfer-induced 3D/2D hybrid perovskites suppress ion migration and reduce luminance overshoot, Nat. Commun 11 (2020) 3378, https://doi.org/10.1038/s41467-020-17072-0.
[58] D.G. Zheng, D.H. Kim, Degradation mechanisms of perovskite light-emitting diodes under electrical bias, Nanophotonics 12 (2023) 451–476, https://doi.org/10.1515/nanoph-2022-0569.
[59] Z. Chen, C. Zhang, X.F. Jiang, M. Liu, R. Xia, T. Shi, D. Chen, Q. Xue, Y.J. Zhao, S. Su, H.L. Yip, Y. Cao, High-performance color-tunable perovskite light emitting devices through structural modulation from bulk to layered film, Adv Mater 29 (2017) 1603157.
[60] A. Sadhanala, S. Ahmad, B. Zhao, N. Giesbrecht, P.M. Pearce, F. Deschler, R. L. Hoye, K.C. Godel, T. Bein, P. Docampo, S.E. Dutton, M.F. De Volder, R.H. Friend, Blue-green color tunable solution processable organolead chloride-bromide mixed halide perovskites for optoelectronic applications, Nano Lett 15 (2015) 6095–6101.
[61] Y.H. Zhou, Y.H. Lou, X.Q. Wang, K.L. Wang, J. Chen, C.H. Chen, Z.K. Wang, Spectral Stable Blue Perovskite Light-Emitting Diodes by Introducing Organometallic Ligand, Adv. Opt. Mater 10 (2021) 2101655, https://doi.org/10.1002/adom.202101655.